Controlling of Transformation Temperatures of Cu–Al–Mn Shape Memory Alloys by Chemical Composition

C. Aksu Canbay[a,*], Z. Karagoz[b] and F. Yakuphanoglu[a]
[a]Department of Physics, Faculty of Science, University of Firat, TR-23119, Elazig, Turkey
[b]Department of Chemistry, Faculty of Science, University of Firat, TR-23119, Elazig, Turkey

(Received November 5, 2013)

The Cu–Al–Mn shape memory alloys having various chemical compositions were prepared by arc melting method to control the phase transformation parameters. The phase transformation parameters and structural properties of the alloys were investigated by differential scanning calorimetry and optic microscopy, respectively. The effects of the chemical composition on characteristic transformation temperatures, enthalpy and entropy values of Cu–Al–Mn ternary system were investigated. The characteristic transformation temperatures of austenite and martensite phase (A_s, A_f, M_s, and M_f) are increased with change in the chemical composition of the alloys. The average crystallite size for the alloys was calculated to determine the effect of aluminum and manganese compositions on the transformation temperatures. The change in transformation temperatures indicates the same trend with change in crystallite size. The obtained results suggest that the phase transformation parameters of the Cu–Al–Mn alloys can be controlled by Al and Mn contents.

DOI: 10.12693/APhysPolA.125.1163
PACS: 62.20.fg, 65.40.–b

1. Introduction

The behavior of advanced materials such as shape memory alloys (SMAs) is significant under various thermal and mechanical conditions due to the thermoelastic martensitic transformation, which occurs in most of these materials. Thermoelastic martensitic transformation is first-order solid–solid phase transformation and is explained by the collective motion of atoms [1, 2]. During the transformation, temperature hysteresis (A_f–M_s) proceeds from the absorption of the internal energy described by three mechanisms: (i) dissipation of energy due to internal friction, (ii) storage of energy, (iii) heat transfers due to the latent heat of phase change [3–6]. The technical importance of SMAs is based on the properties such as high damping capacity, pseudoelasticity (PE) and shape memory effect (SME). In Cu-based SMAs, unique thermomechanical properties derive from the thermoelastic martensitic transformation and depend on crystal structures of the phases involved in transformation process. Cu-based SMAs exhibit a martensitic transformation on cooling and austenite transformation on heating and during cooling process, close-packed structures are characterized by long period stocking order such as 6R, 18R, and 2H type structures [7–10].

To our knowledge, there is not any study on effects of chemical composition on shape memory parameters of CuAlMn with higher manganese and lower aluminum content. Thus, our aim is to investigate the change in phase transformation temperatures, thermodynamic parameters and microstructure properties of CuAlMn alloys.

*corresponding author; e-mail: caksu@firat.edu.tr

2. Experimental

Cu–Al–Mn shape memory polycrystalline alloys with nominal compositions given in Table I were produced by arc melting. The specimens were solution-treated at 1123 K for 1 h and quenched in iced-brine water. The characteristic transformation behaviors and kinetic parameters were determined by Shimadzu DSC-60A differential scanning calorimetry. The chemical compositions of the alloys were determined by LEO evo 40 Model energy dispersive X-ray (EDX). The phases present in the polycrystalline samples were determined by Rigaku RadB-DMAX II diffractometer with Cu K_α radiation at room temperature. The microstructure and morphology of martensites formed in samples were observed using Nikon MA200 model optical metallographic microscope.

TABLE I
Chemical compositions of the alloys.

Alloy ID	Chemical compositions [at.%]		
	Cu	Al	Mn
CAM1	70.38	26.56	3.06
CAM2	67.45	27.96	4.60
CAM3	72.50	24.70	2.81
CAM4	74.15	20.28	5.57

3. Results and discussion

3.1. Structural properties of the Cu–Al–Mn alloys

X-ray diffraction patterns of the alloys are shown in Fig. 1. The main diffraction peaks of martensite phase observed in samples were found to be (122), (0022), (128), (1210) and (042).

The X-ray results indicate that the prepared alloys are polycrystalline. The polycrystalline Cu–Al–Mn alloys

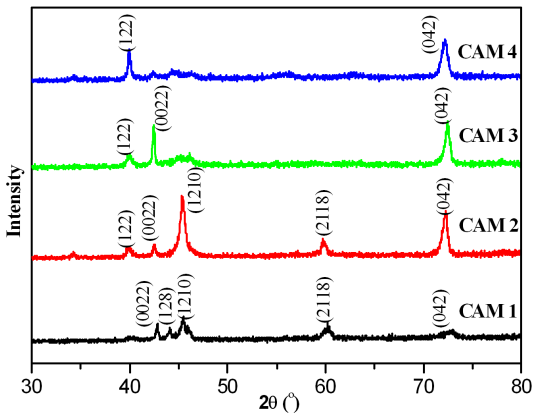

Fig. 1. X-ray diffraction patterns of the CAM1, CAM2, CAM3, and CAM4 samples.

with different compositions, after solution and quenching treatment, experience the thermoelastic martensite transformation, $(L2_1) \rightarrow (18R)$. The martensite reorientation under external force causes a thermoelastic martensite transformation and in turn, the alloys exhibit the shape memory effect. The microstructure of the alloys was analyzed by optical microscopy observations and optic images of the alloys are given in Fig. 2. As seen in Fig. 2, the martensite variants, grains, and grain boundaries occur in the structure of the each sample.

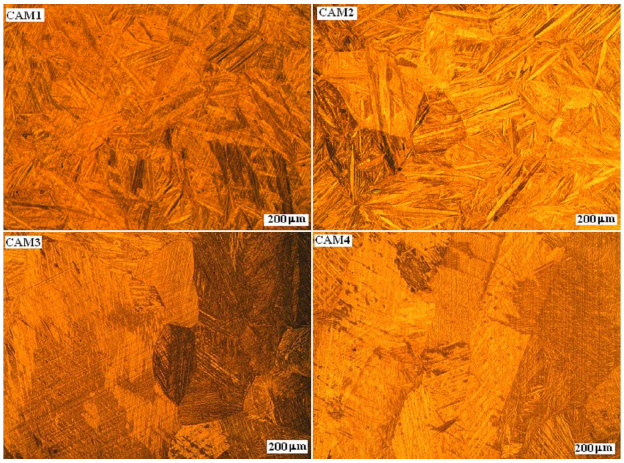

Fig. 2. Optical micrographs of the CAM1, CAM2, CAM3, and CAM4 samples.

The morphology of the alloys were changed with variation in aluminum and manganese contents. To analyze the effects of crystallize size on transformation temperatures of the alloys, we determined crystallite size (D) for each sample by the Debye–Scherrer equation [11, 12].

$$D = \frac{0.9\lambda}{B_{1/2}\cos\theta}, \tag{1}$$

where λ is the wavelength of the X-ray (Cu K_α radiation), B is the peak full width at half maximum and θ is the Bragg angle. The crystallite size for the alloys were calculated by means of Eq. (1) and the crystallite size was plotted as a function of transformation temperatures and are given in Fig. 3.

As seen in Fig. 4, the phase transformation temperatures (M_s, A_s) exhibits the similar trend with crystallite size. This indicates that the crystallite size affects the phase transformation temperatures.

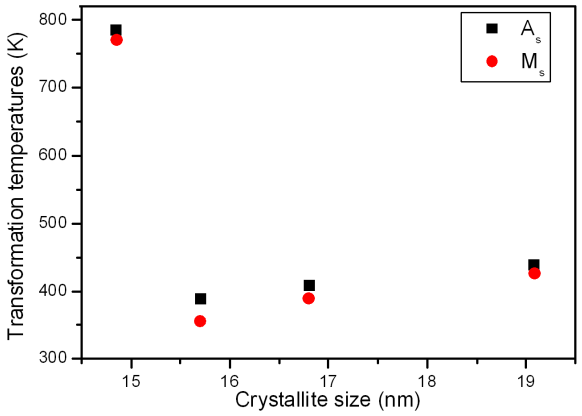

Fig. 3. Variation of transformation temperatures with crystallite size.

3.2. Thermal properties of the Cu–Al–Mn alloys

We have analysed phase transformation behavior with differential scanning calorimetry measurements. The DSC measurements for heating and cooling were performed with a heating/cooling rate of 25 K/min and obtained DSC plots of the Cu–Al–Mn alloys were shown in Fig. 4. The characteristic transformation temperatures such as A_s, A_f, M_s, and M_f of the alloys were determined from Fig. 4 and are given in Table II. As seen in Fig. 4, DSC curves give the large exothermic and endothermic peaks, which is in good correspondence with martensitic and reverse transformations at around 340–470 K for samples CAM1, CAM2, CAM3, and 720–820 K for CAM4 sample. The transformation temperatures of the studied alloys are higher than that of Cu–20.4Al–8.7Mn (at.%) and Cu–25.3Al–4.1Mn (at.%) alloys [13]. Whereas the temperatures of CAM1, CAM2, CAM3 shape memory alloys are lower than that of Cu–11.9Al–2.5Mn (wt%) shape memory alloys produced by sintering-evaporation process and the CAM4 alloy has the high transformation temperature [14]. These results indicate that the transformation temperatures for austenite and martensite phase vary with the variation in aluminum and manganese contents in the copper matrix. The change in A_s–M_s hysteresis is important to determine the shape memory effect. Because whatever the hysteresis is narrow, shape memory effect is high [15]. On the basis of this, the hysteresis value (A_s–M_s) versus manganese concentration is shown in Fig. 5. As seen in Fig. 5, the hysteresis value is changed with manganese content.

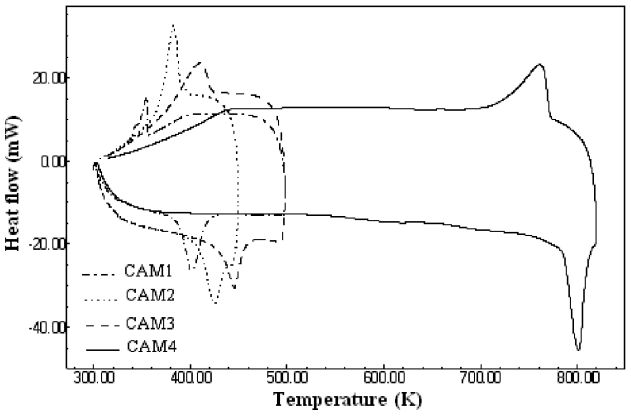

Fig. 4. DSC curves of CAM1, CAM2, CAM3, and CAM4 samples with a heating/cooling rate of 25 K/min.

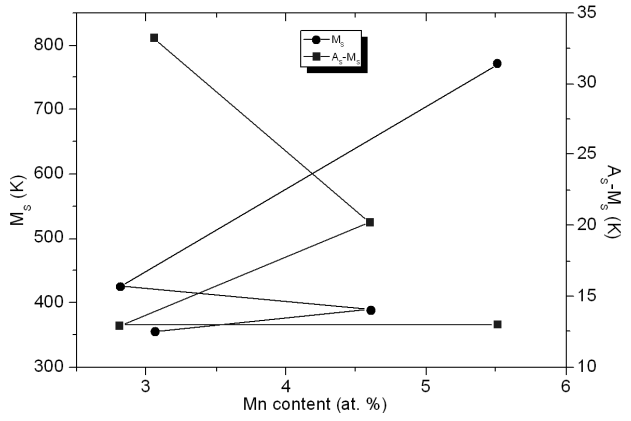

Fig. 5. Variation of Mn content with M_s temperature and temperature hysteresis.

Figure 6 shows variation of Al content with M_s temperature and temperature hysteresis. As seen in Fig. 6, with increasing Al content up to 25 at.%, M_s temperature decreases and then slight decrease was observed. A sudden decrease in M_s temperature is due to decrease in crystallite size. In addition to crystallite size, it is well known that the alloy composition is an important effect on the change of M_s temperature. Whereas, temperature hysteresis is increased with Al content and after 28 at.% Al content, it decreases suddenly. These results suggest that the transformation temperatures are changed with the crystallite size and alloy composition. Enthalpy ΔH values of phase transformation were determined from DSC curves using tangent method and are given in Table II. As seen in Table II, the ΔH value is changed with alloy composition. The relation between transformation energy and thermodynamic equilibrium temperature can be written as [16]:

$$\Delta S_{M\to A} = \frac{\Delta H_{M\to A}}{T_0}, \tag{2}$$

where ΔS is the entropy change, ΔH is the enthalpy change, and T_0 is the equilibrium temperature between martensite and austenite phases calculated by the relation of $T_0 = (A_\mathrm{f} + M_\mathrm{s})/2$ [17]. The ΔS values were determined by Eq. (2) and are given in Table II. The ΔS values of the alloys were changed by alloy composition. It is seen that the shape memory behavior of the alloys depends on thermodynamic parameters.

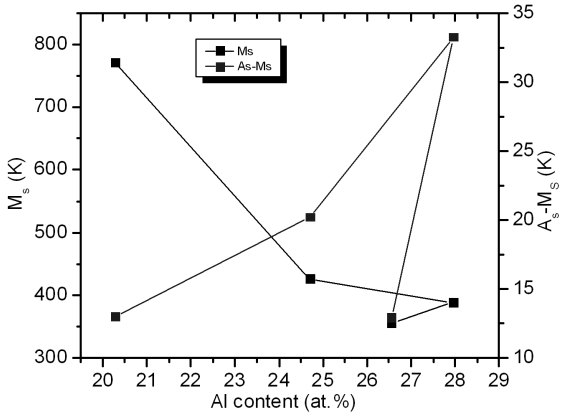

Fig. 6. Variation of Al content with M_s temperature and temperature hysteresis.

TABLE II

Thermodynamic and kinetic parameters of CAM1, CAM2, CAM3, and CAM4 samples with a heating rate of 25 K/min.

Alloy ID	A_s [K]	A_f [K]	M_s [K]	M_f [K]	$(A_\mathrm{s}$–$M_\mathrm{s})$ [K]	T_0 [K]	$\Delta H_{M\to A}$ [J g^{-1}]	$\Delta S_{M\to A}$ [J g^{-1} K^{-1}]
CAM1	388.93	414.36	355.66	347.55	33.27	385.01	7.86	0.020
CAM2	409.32	434.25	389.1	372.42	20.22	411.67	4.19	0.010
CAM3	438.76	465.78	425.82	411.85	12.94	445.8	6.83	0.015
CAM4	784.74	808.25	771.73	723.79	13.01	789.69	11.09	0.014

We have determined the kinetic parameters such as activation energy on the basis of DSC results. For this, we used Kissinger method given by [18]:

$$\mathrm{d}\left[\ln\left(\phi/T_\mathrm{m}^2\right)\right]/\mathrm{d}(1/T) = -E/R, \tag{3}$$

where ϕ is the heating rate, T_m is the maximum temperature of the DSC peak, R is the universal gas constant

and E is the activation energy. To calculate activation energy of phase transformation, we plotted the curves of $\ln(\phi/T_m^2)$ vs. $1000/T$ shown in Fig. 7. The activation energy values were determined from the slope of Fig. 7 and the activation energy values of the CAM1, CAM2, CAM3, and CAM4 samples were found to be 108.156, 195.54, 181.87, and 305.24 kJ/mol, respectively. The activation energy value for the alloys is increased with Al and Mn contents. This indicates that Al and Mn contents increase the phase transformation temperatures.

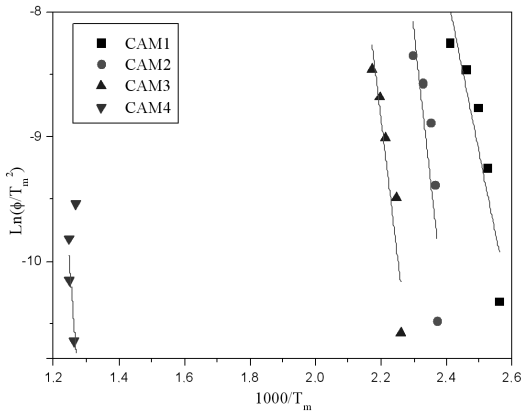

Fig. 7. Activation energy curves of CAM1, CAM2, CAM3, and CAM4 samples.

4. Conclusions

The Cu–Al–Mn shape memory alloys having various chemical compositions were prepared by arc melting method. The phase transformation temperatures, enthalpy, and entropy values of Cu–Al–Mn ternary system were determined. It was found that the phase transformation temperatures of the alloys were changed by alloy composition. The change in phase transformation temperature was explained on the basis of crystallite size and alloy composition. The obtained results suggest that the phase transformation parameters of the Cu–Al–Mn alloys can be controlled by crystallite size and metal contents in matrix.

References

[1] H.H. Kart, M. Tomak, M. Uludoğan, T. Cagın, *Comput. Mater. Sci.* **32**, 107 (2005).

[2] Z. Wang, G. Zu, T. Xo, Y. Huo, *Thermochim. Acta* **436**, 153 (2005).

[3] P. Entel, R. Meyer, K. Kadau, *Philos. Mag. B* **80**, 183 (2000).

[4] A. Chryochoos, H. Pham, O. Maisonneuve, *Nucl. Eng. Des.* **162**, 1 (1996).

[5] S. Kazanc, C. Tatar, *Int. J. Solids Struct.* **45**, 3282 (2008).

[6] F. Gori, D. Carnevale, A. Doro Altan, S. Nicosia, E. Pennestri, *Int. J. Thermophys.* **27**, 866 (2006).

[7] V.V. Kokorin, L.E. Kozlova, A.O. Perekos, *Mater. Sci. Eng. A* **481-482**, 542 (2008).

[8] U.S. Mallik, V. Sampath, *J. Alloys Comp.* **459**, 142 (2008).

[9] M. Sharma, S.K. Vajpai, R.K. Dube, *Powder Metall.* **54**, 620 (2011).

[10] K. Matsushita, T. Okomoto, T. Okamoto, *J. Mater. Sci.* **20**, 689 (1985).

[11] N. Suresh, U. Ramamurty, *J. Alloy Comp.* **449**, 113 (2008).

[12] D. Sonia, P. Rotaru, S. Rizescu, N.G. Bizdoaca, *J. Therm. Anal. Calorim.* **111**, 1255 (2013).

[13] N. Zárubová, V. Novák, *Mater. Sci. Eng. A* **378**, 216 (2004).

[14] S. Gong, Z. Li, G.Y. Xu, N. Liu, Y.Y. Zhao, S.Q. Liang, *J. Alloys Comp.* **509**, 2924 (2011).

[15] C. Aksu Canbay, Ph.D Thesis, Fırat University, Institue of Science, Elazığ, Turkey 2010.

[16] M.O. Prado, P.M. Decarte, F. Lovey, *Scr. Metall. Mater.* **33**, 878 (1995).

[17] R.J. Salzbrenner, M. Cohen, *Acta Metall.* **27**, 739 (1979).

[18] H.E. Kissinger, *Anal. Chem.* **29**, 1702 (1957).